

Melting of Zn nanoparticles embedded in SiO₂ at high temperatures: Effects on surface plasmon resonances

H. Amekura, M. Tanaka, Y. Katsuya, H. Yoshikawa, H. Shinotsuka, S. Tanuma, M. Ohnuma, Y. Matsushita, K. Kobayashi, Ch. Buchal, S. Mantl, and N. Kishimoto

Citation: *Appl. Phys. Lett.* **96**, 023110 (2010);

View online: <https://doi.org/10.1063/1.3290984>

View Table of Contents: <http://aip.scitation.org/toc/apl/96/2>

Published by the [American Institute of Physics](#)

Articles you may be interested in

[Melting-solidification transition of Zn nanoparticles embedded in SiO₂: Observation by synchrotron x-ray and ultraviolet-visible-near-infrared light](#)

Journal of Applied Physics **108**, 104302 (2010); 10.1063/1.3494098



SciLight

Sharp, quick summaries **illuminating**
the latest physics research

Sign up for **FREE!**

AIP
Publishing

Melting of Zn nanoparticles embedded in SiO₂ at high temperatures: Effects on surface plasmon resonances

H. Amekura,^{1,a)} M. Tanaka,² Y. Katsuya,³ H. Yoshikawa,² H. Shinotsuka,⁴ S. Tanuma,⁴ M. Ohnuma,⁵ Y. Matsushita,² K. Kobayashi,² Ch. Buchal,⁶ S. Mantl,⁶ and N. Kishimoto¹

¹*Ion Beam Group, National Institute for Materials Science (NIMS), 3-13 Sakura, Tsukuba, Ibaraki 305-0003, Japan*

²*NIMS Beamline Station at SPring-8, National Institute for Materials Science (NIMS), 1-1-1 Kouto, Sayo-cho, Hyogo 679-5148, Japan*

³*SPring-8 Service Co. Ltd., 1-1-1 Kouto, Sayo-cho, Hyogo 679-5148, Japan*

⁴*Nano Characterization Center, National Institute for Materials Science (NIMS), 1-2-1 Sengen, Tsukuba, Ibaraki 305-0047, Japan*

⁵*Neutron Scattering Group, National Institute for Materials Science (NIMS), 1-2-1 Sengen, Tsukuba, Ibaraki 305-0047, Japan*

⁶*Institut fuer Bio- und Nanosysteme (IBN1-IT), Forschungszentrum Juelich GmbH, D-52425 Juelich, Germany*

(Received 31 August 2009; accepted 16 December 2009; published online 14 January 2010)

Zn nanoparticles at room temperature show two absorption peaks in the near-infrared (NIR) and the ultraviolet (UV) regions, both of which satisfy the criterion of surface plasmon resonance (SPR). From x-ray diffraction at high temperatures, it was found that the Zn nanoparticles in SiO₂ melt at 360–420 °C and solidify at 250–310 °C with a large temperature hysteresis. While the NIR peak disappears with melting, the UV peak shows sudden energy shift with melting but survives even after the melting. The first-principle band calculation ascribes the UV and NIR peaks to SPR-enhanced inter- and intraband transitions, respectively. © 2010 American Institute of Physics. [doi:10.1063/1.3290984]

Surface plasmon resonance (SPR) of metal nanoparticles (NPs) embedded in insulators is receiving considerable attention because of possible applications to ultra-fast optical nonlinear devices,¹ one-molecule detection by enhanced Raman spectroscopy,² and plasmonics.³ For these applications, NPs should properly work even under strong heat load due to high-intensity laser irradiation. Melting of NPs by heat and effects on the SPR are important issues to be clarified. Although there are many studies on melting of NPs,^{4–9} only very limited numbers of studies are reported concerning the melting effects on the SPR of metal NPs such as Au¹⁰ and Cu¹¹ in transparent insulators.

Although these publications^{10,11} included exciting interpretation of the absorption spectra, the results are not free from criticism because they did not determine the melting point (T_{mp}) of the NPs experimentally but presumed the T_{mp} value from data in past literature. However, T_{mp} of NPs embedded in a solid matrix is difficult to predict, because reduction of NP size decreases but the pressure from the matrix increases the T_{mp} . Since both of these effects contribute to T_{mp} in different ways, experimental determination of T_{mp} is essential for embedded NPs. In this letter, we describe a study in which we experimentally determined the temperature dependences of both the x-ray diffraction (XRD), i.e., T_{mp} , and the SPR absorption of Zn NPs embedded in silica glass (SiO₂). Furthermore, the occurrence of little change in size of the NPs during high-temperature (HT) measurements was experimentally confirmed by laboratory-scale small-

angle x-ray scattering (lab-SAXS), since changes in the size of NPs during the HT measurements cause difficulty in interpretation of the results.

Zinc NPs are attractive because these NPs exhibit two SPR peaks at around 1.2 and 4.8 eV,¹² i.e., one in the near-infrared (NIR) region and the other in the ultraviolet (UV) region. Both of these peaks satisfy the criterion of SPR:

$$|\varepsilon^{\text{Zn}}(\omega) + 2\varepsilon^{\text{SiO}_2}(\omega)| = (\text{local})\text{minimum}, \quad (1)$$

where $\varepsilon^{\text{Zn}}(\omega)$ and $\varepsilon^{\text{SiO}_2}(\omega)$ denote complex dielectric functions of Zn and SiO₂, respectively.¹²

Zn NPs were formed in KU-1 type SiO₂ substrate by implantation of Zn ions of 60 keV up to a fluence of 1.0×10^{17} ions/cm². The formation parameters were the same as those reported in our previous study.^{13,14} We applied the glancing incident angle XRD (GIXRD) method to monitor the solid-liquid (SL) transition of Zn NPs. However, because an excessively long measurement duration at HTs might cause coarsening of the NPs, we used a high-intensity x-ray from a synchrotron radiation (SR) facility to shorten the measurement duration. A HT sample holder was installed in the vacuum chamber of the high-resolution diffractometer¹⁵ of the BL15XU beamline at the SPring-8 SR facility. The sample was kept in a vacuum to avoid oxidation during the HT measurements. An x-ray energy of 5.414 keV was used. Diffraction patterns were recorded by a YAP detector with scanning at a scattering angle of 2θ , where the incident angle θ was fixed at 3°.

Figure 1(a) shows the temperature dependence of the Zn (101) diffraction peak detected by SR-GIXRD. The upward and downward triangles show data points taken in the rising- and falling-temperature sequences, respectively. With in-

^{a)} Author to whom correspondence should be addressed. Electronic mail: amekura.hiroshi@nims.go.jp. FAX: +81-29-863-5599. Tel.: +81-29-863-5479.

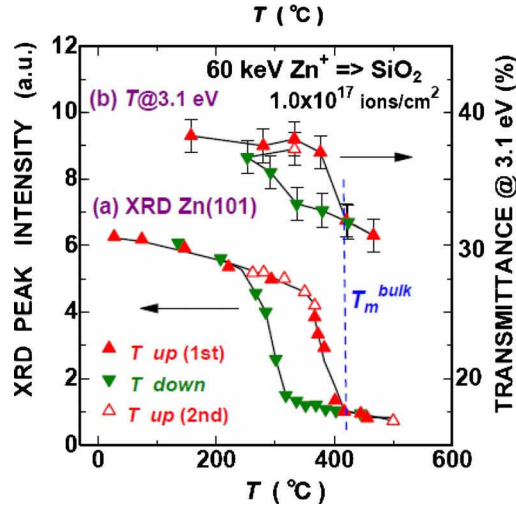


FIG. 1. (Color online) Temperature dependence of (a) the peak intensity of Zn (101) diffraction from Zn NPs embedded in SiO₂ detected by SR-GIXRD, and of (b) the optical transmittance T detected at a fixed photon energy of 3.1 eV. The upward and downward triangles show data points taken in the rising- and falling-temperature sequences, respectively. The closed and open upward triangles show data taken in the first and second runs, respectively. The solid lines are guides for the eye. The dashed line indicates the melting point of bulk Zn.

creasing temperature, the intensity shows a gradual decrease until ~ 360 °C and then decreases steeply. The steep decrease is completed at around 418 °C, which is very close to the bulk T_{mp} of 419.6 °C. The steep decrease in the diffraction intensity is ascribed to the melting of Zn NPs. On the other hand, in the falling sequence the intensity maintains a low value that corresponds to the molten phase even when the temperature falls to ~ 310 °C, then shows a steep increase as the temperature falls further to ~ 250 °C. A temperature hysteresis with a width of ~ 110 °C was observed. After solidification was completed in the falling sequence, the temperature was increased again (second run). The data for the second run are indicated by open triangles in the figure. The second-run data show a close correspondence with the curve of the first-run data, confirming that the hysteresis was not due to spurious effects but reproducible.

The size distributions of the Zn NPs before and after the GIXRD measurements at HTs were determined by the lab-SAXS measurements.¹⁶ The mean diameter was respectively 11.0 and 12.0 nm before and after the measurements, indicating that coarsening of the NPs during the measurements is negligible. It should be noted that temperature hysteresis is a relatively common phenomenon in the SL transitions of embedded NPs.⁷⁻⁹ Since the SL transition is one of the 1st order phase transitions, large hysteresis is a natural consequence. However, in continuous thin-films and bulk materials, the large hysteresis is hindered by the heterogenous nucleation due to imperfections. Once the heterogenous nucleation happens at any parts of the materials, all the parts suffer the transition because any parts are connected with each other. Contrary, embedded NPs are separated from each other by matrix, i.e., SiO₂. In this case, even if the heterogenous nucleation happens in some embedded NPs, the nucleation does not propagate to the other NPs. Consequently the large hysteresis is observed.

Optical transmission spectroscopy was carried out at HTs in the wavelength region of 215–1700 nm with a resolution of 2 nm in our laboratory, using a conventional

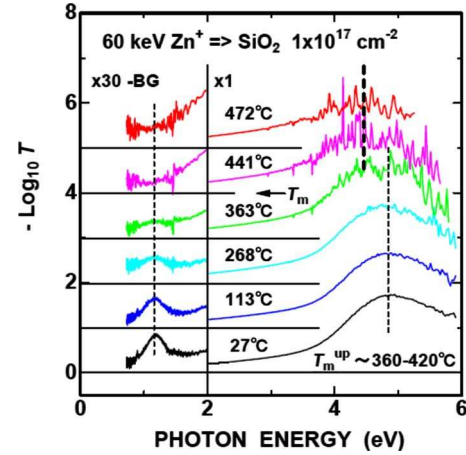


FIG. 2. (Color online) Temperature dependence of the optical density spectra, i.e., $-\text{Log}_{10} T$, in the near-infrared (NIR), visible, and ultraviolet (UV) regions, where T denotes the optical transmittance. The spectra in the NIR region were magnified 30 times and the backgrounds were subtracted.

double-beam spectrometer equipped with a HT vacuum sample chamber. The optical density spectra detected in the rising-temperature sequence are shown in Fig. 2. With increasing temperature, the NIR peak at 1.2 eV gradually decreases in height and increases in width. The NIR peak is faintly visible at 363 °C, but is no longer visible at 441 °C. Since the XRD peak steeply decreases between 360 and 420 °C, the disappearance of the NIR peak can be considered to be coincident with the melting. On the contrary, the UV peak around 4.8 eV survives even at higher temperatures than 420 °C where the XRD data show the melting of all of the Zn NPs.

While the UV peak energy hardly changes from 4.8 eV even with heating from RT to ~ 330 °C, the peak suddenly shifts to ~ 0.3 eV lower energy with the occurrence of melting. Since the melting is a transition from the crystalline phase to the liquid phase, i.e., similar to the amorphous phase, the energy shift of the optical transition is quite acceptable. In fact, shifts of band-gap energies are reported in some nonmetallic solids with the transition from a crystalline phase to a solid amorphous phase.^{17,18} It should be noted that although there are many sharp lines superimposed on the broad UV peak at HTs, they are artifacts because they have no reproducibility in terms of positions and intensities.

To confirm that the shift of the UV peak is due to melting, the temperature dependence of the UV peak was evaluated in both the rising- and falling-temperature sequences. In addition to the sudden shift of the peak energy, the low-energy shoulder of the UV peak also showed a similar sudden shift with melting. Since the peak is broad and noisy, the determination of the peak energy includes large uncertainty. Instead of the peak energy, the transmittance value at a fixed energy in the tail region of the UV peak, e.g., 3.1 eV, where the S/N ratio is relatively better, can serve as a more useful measure of the energy shift. As shown in Fig. 1(b), the transmittance at 3.1 eV exhibited an almost constant value of $\sim 38\%$ up to ~ 375 °C in the rising sequence and then steeply decreased at higher temperatures. This is due to the sudden low-energy shift of the UV peak, which is a consequence of the melting of the Zn NPs. In the falling sequence, a low transmittance value was maintained down to ~ 335 °C then the value returned to a high level. Temperature hysteresis was also observed in the optical absorption, which was

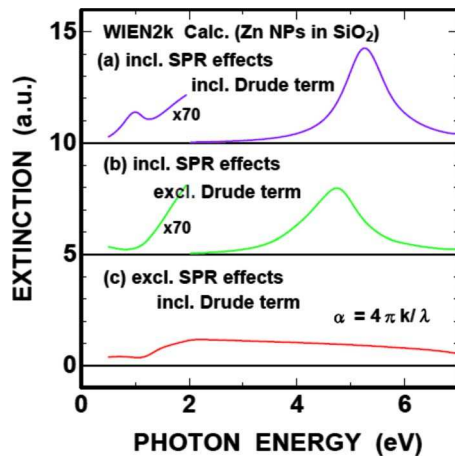


FIG. 3. (Color online) Theoretical optical extinction spectra of Zn NPs in SiO_2 derived by the first principle band calculation code WIEN2K. In (a) and (b), the depolarization effects, i.e., the field enhancement effects due to SPR, of metal NPs are included using the 1st order Mie formula. In (b), the Drude term is artificially excluded. In (c), the SPR effects are excluded, i.e., the extinction α is derived from $\alpha = 4\pi k/\lambda$, instead of the Mie formula, where k denotes the imaginary part of the complex refractive index.

similar to that observed in the XRD results shown in Fig. 1(a).

To understand the different temperature dependences between the NIR and UV peaks, the origins of these two peaks were evaluated using *ab initio* band calculation code WIEN2K.¹⁹ The code calculated the band diagram and the complex dielectric function of bulk Zn, which consists of two different components, i.e., the intraband (Drude) and the interband contributions.²⁰ Theoretical absorption spectra of Zn NPs embedded in SiO_2 were derived from the dielectric function using the first order Mie formula,²¹ which includes the depolarization effect of metal NPs in insulator. The relaxation frequency \hbar/τ in the Drude term was substituted by a larger value of 1 eV in order to take account for the mean-free-path (MFP) reduction due to the NP confinement. The result is shown in Fig. 3(a): Two peaks are observed at 1.0 and 5.3 eV, both of which are in good agreement with the experimental peaks at 1.2 and 4.8 eV, respectively. If the Drude term is neglected, the NIR peak disappears but the UV peak remains with a certain low-energy shift, as shown in Fig. 3(b). From the band-diagram and these facts, the NIR and UV peaks are ascribed to intraband and $4s$ - $4p$ interband transitions, respectively.

Since the intraband electrons have free-electron-like nature, they are more sensitive to reduction of the MFP of conduction electrons.²¹ Coincident with the melting, the MFP is steeply reduced to the order of the lattice constant and the NIR peak is strongly damped and disappears. Contrary, the UV peak has the interband transition nature; i.e., is free from the Drude-like strong damping even after the melting.

It should be noted again that the UV peak is also due to the SPR: The energy of the UV peak does not match with any of special band singularities. Thus, the band structure is not the direct reason why the UV peak appears. In fact, the calculated joint-density-of-states (JDOS) shows a featureless spectrum in the region of 2–6 eV. As one of the trials, the bulk absorption formula $\alpha = 4\pi k/\lambda$ was used instead of Mie formula in order to exclude the field-enhancement effect of the NP structure. The result is shown in Fig. 3(c). The UV

peak does not appear but only weak feature-less absorption is observed. Thus, the UV peak is also a consequence of the SPR effects. In fact, the UV peak satisfies the SPR criterion (1).

Several years ago, we discussed a similar problem, i.e., the identification of SPR from two absorption peaks at 3.3 and 6.0 eV of Ni NPs in SiO_2 .²² From numerical calculation of the size dependence of the extinction spectra, we tentatively concluded that the peak which was more strongly suffered by the MFP reduction, i.e., the 3.3 eV peak, was ascribed to the SPR. Now the opinion has been changed: Even in the interband transition regions, appearance of the peak can be due to the field enhancement effect of SPR. Consequently, all the peaks which satisfy the criterion (1) are SPRs. This is not only a small change of the viewpoint, but may bring fruitful new phenomena: UV peaks of metal NPs which were believed due to the interband transitions may show new plasmonic phenomena.

A part of this study was granted from The Murata Science Foundation. The authors thank the staffs of BL15XU, NIMS, and of SPring-8 for their help at the beamline. The GIXRD measurements at HT were performed under the approval of NIMS Beamline Station (Proposal Nos. 2006B4501, 2007A4501, and 2007B4502).

¹R. F. Haglund, L. Yang, R. H. Magruder, C. W. White, R. A. Zuhr, L. Yang, R. Dorsinville, and R. R. Alfano, *Nucl. Instrum. Methods Phys. Res. B* **91**, 493 (1994).

²S. Nie and S. R. Emory, *Science* **275**, 1102 (1997).

³H. A. Atwater, S. Majer, A. Polman, J. A. Dionne, and L. Sweatlock, *MRS Bull.* **30**, 385 (2005).

⁴M. Takagi, *J. Phys. Soc. Jpn.* **9**, 359 (1954).

⁵P. Buffat and J.-P. Borel, *Phys. Rev. A* **13**, 2287 (1976).

⁶S. E. Donnelly, R. C. Birtcher, C. W. Allen, I. Morrison, K. Furuya, M. Song, K. Mitsuishi, and U. Dahmen, *Science* **296**, 507 (2002).

⁷Q. Xu, I. D. Sharp, C. W. Yuan, D. O. Yi, C. Y. Liao, A. M. Glaeser, A. M. Minor, J. W. Beeman, M. C. Ridgway, P. Kluth, J. W. Ager III, D. C. Chrzan, and E. E. Haller, *Phys. Rev. Lett.* **97**, 155701 (2006).

⁸M. A. Tagliente, G. Mattei, L. Tapfer, M. V. Antisari, and P. Mazzoldi, *Phys. Rev. B* **70**, 075418 (2004).

⁹H. H. Andersen and E. Johnson, *Nucl. Instrum. Methods Phys. Res. B* **106**, 480 (1995).

¹⁰D. Dalacu and L. Martinu, *Appl. Phys. Lett.* **77**, 4283 (2000).

¹¹O. A. Yeshchenko, I. M. Dmitruk, A. A. Alexeenko, and A. M. Dmytruk, *Phys. Rev. B* **75**, 085434 (2007).

¹²H. Amekura, N. Umeda, K. Kono, Y. Takeda, N. Kishimoto, C. Buchal, and S. Mantl, *Nanotechnology* **18**, 395707 (2007).

¹³H. Amekura and N. Kishimoto, in *Lecture Notes in Nanoscale Science and Technology*, edited by Z. Wang (Springer, New York, 2009), Vol. 5, Chap. 1.

¹⁴H. Amekura, N. Umeda, Y. Sakuma, N. Kishimoto, and C. Buchal, *Appl. Phys. Lett.* **87**, 013109 (2005).

¹⁵T. Ikeda, A. Nisawa, M. Okui, N. Yagi, H. Yoshikawa, and S. Fukushima, *J. Synchrotron Radiat.* **10**, 424 (2003).

¹⁶H. Amekura, M. Ohnuma, N. Kishimoto, C. Buchal, and S. Mantl, *J. Appl. Phys.* **104**, 114309 (2008).

¹⁷P. A. Stolk, F. W. Saris, A. J. M. Berntsen, W. F. van der Weg, L. T. Sealy, R. C. Barklie, G. Krotz, and G. Muller, *J. Appl. Phys.* **75**, 7266 (1994).

¹⁸S. Kondo, H. Tanaka, and T. Saito, *Solid State Commun.* **112**, 665 (1999).

¹⁹P. Blaha, K. Schwarz, G. K. H. Madse, D. Kvasnicka, and J. Luitz, WIEN2K (Technische Universität Wien, Austria, 2001).

²⁰C. Ambrosch-Draxl and J. O. Sofo, *Comput. Phys. Commun.* **175**, 1 (2006).

²¹U. Kreibig and M. Vollmer, *Optical Properties of Metal Clusters* (Springer, Berlin, 1995).

²²H. Amekura, Y. Takeda, and N. Kishimoto, *Nucl. Instrum. Methods Phys. Res. B* **222**, 96 (2004).